arXiv:cond-mat/0506364v1 [cond-mat.supr-con] 15 Jun 2005

Correlated Band Structure and the Ground-State Phase Diagram in High-T_C Cuprates

Werner Hanke [a,*], Markus Aichhorn [b], Enrico Arrigoni [b], Michael Potthoff [a]

[a] *Institute for Theoretical Physics, University of Würzburg, Am Hubland, 97074 Würzburg, Germany*

[b] *Institute for Theoretical Physics and Computational Physics, Graz University of Technology, Petersgasse 16, 8010 Graz, Austria*

Abstract

We review results obtained with a recently proposed variational cluster approach (VCA) for the competition between d-wave superconductivity (dSC) and antiferromagnetism (AF) in the high-T_C cuprates. Comparing the single-particle spectra of a two-dimensional Hubbard model with quantum Monte-Carlo (QMC) and experimental data, we verify that the VCA correctly treats the low-energy excitations. The cluster calculations reproduce the overall ground-state phase diagram of the high-temperature superconductors both for electron- and hole-doping. In particular, they include salient features such as the enhanced robustness of the AF state in case of electron doping. For electron- but also for hole-doping, we clearly identify a tendency to phase separation into a mixed AF-dSC phase at low and a pure dSC-phase at high doping.

Key words: superconductivity, antiferromagnetism, electron and hole doping
PACS: 71.10.Hf; 71.27.+a; 75.30Mb

The central issue in the field of high-temperature superconductivity (HTSC) is the connection of the microscopic interactions at the level of electrons and ions, which are at high energy and temperature T, with the "emerging phenomena" at $T = 0$, i.e. competing and nearly degenerate orders – antiferromagnetism (AF), d-wave superconductivity (dSC), heterogeneous phases, etc. We will not go into a lengthy discussion of what interactions should be retained at the electron-ion level. But, when choosing the two-dimensional ($2D$) one-band Hubbard model, i.e.

$$H = \sum_{i,j} t_{i,j} c_i^\dagger c_j + U \sum_i n_{i,\uparrow} n_{i,\downarrow} \,, \qquad (1)$$

where $t_{i,j}$ denote hopping matrix elements, $n_{i,\uparrow}$ the density at site i with spin "↑" and U the local Coulomb repulsion, one has introduced gross simplifications, leaving out other orbital (e.g. p) degrees of freedom, long-range Coulomb interaction, electron-phonon coupling, etc [1]. Nevertheless, this model choice appears to be legitimate, last not least in view of the amazing agreement achieved between numerical simulations and experimental results for the normal-state properties of the cuprates [2,3].

At low temperatures different orders appear, which are not separated by distinct energy scales but compete with each other. What is required is a kind of "magnifying lens" which allows to resolve these competing orders. Ideally, one should employ a systematic renormalization-group approach to integrate out the irrelevant degrees of freedom and, thereby, to correctly bridge high to low energies and eventually to go to $T = 0$. For the strong-correlation case, realized in the HTSC, how to do this is, however, by no means obvious. In this context, cluster techniques provide an alternative way to systematically approach the infinite-

* Corresponding author. Tel: +49 931 888-5714 fax: +49 931 888-5141

Email address: hanke@physik.uni-wuerzburg.de (Werner Hanke).

size (and, thereby, low-energy) limit.

Here, we review progress obtained with the variational cluster approach (VCA), which was proposed and used by Potthoff et. al. [4, 5]. This approach provides a rather general and controlled way to go to the infinite-sized lattice fermion system at low temperatures and at $T = 0$, in particular. The ground-state phase diagram of the $2D$ one-band Hubbard model was calculated within VCA by Sénéchal et. al. [6] and, independently, by two of us [7]. There are certain technical differences, which we discuss below, but the "upshot" of the two works is as follows: For the cluster sizes used in the VCA, the $T = 0$ phase diagram of the Hubbard model (1), with hopping terms up to third-nearest neighbors, correctly reproduces salient features of the HTSC, such as the AF and dSC ground states in doping ranges, which are qualitatively in agreement with electron- and hole-doped cuprates.

The VCA is based on the self-energy-functional approach (SFA) [8]. The SFA provides a variational scheme to use dynamical information from an exactly solvable "reference system" (for example an isolated cluster) to approximate the physics of a system in the thermodynamic limit. For a system with Hamiltonian $H = H_0(\boldsymbol{t}) + H_1(\boldsymbol{U})$ and one-particle and interaction parameters $\boldsymbol{t}$ and $\boldsymbol{U}$, the grand potential is written as a functional of the self-energy $\boldsymbol{\Sigma}$ as

$$\Omega_{\boldsymbol{t},\boldsymbol{U}}[\boldsymbol{\Sigma}] = F_{\boldsymbol{U}}[\boldsymbol{\Sigma}] + \mathrm{Tr}\ln\left(\boldsymbol{G}_{0,\boldsymbol{t}}^{-1} - \boldsymbol{\Sigma}\right)^{-1}, \qquad (2)$$

with the stationary property $\delta\Omega_{\boldsymbol{t},\boldsymbol{U}}[\boldsymbol{\Sigma}_{\mathrm{phys}}] = 0$ for the physical self-energy. Here, $\boldsymbol{G}_{0,\boldsymbol{t}} = (\omega + \mu - \boldsymbol{t})^{-1}$ is the free Green's function at frequency ω, and μ is the chemical potential. $F_{\boldsymbol{U}}[\boldsymbol{\Sigma}]$ is the Legendre transform of the Luttinger-Ward functional and determines the fully interacting Green's function via $\boldsymbol{G} = -\delta F_{\boldsymbol{U}}[\boldsymbol{\Sigma}]/\delta\boldsymbol{\Sigma}$. It is important to note that $F_{\boldsymbol{U}}[\boldsymbol{\Sigma}]$ is a universal functional: The functional dependence is only determined by the interaction parameters $\boldsymbol{U}$ (for example, the Hubbard interaction in Eq. (1)). Therefore, the functional $F_{\boldsymbol{U}}[\boldsymbol{\Sigma}]$ is the same as the functional for a problem which is "simpler" and solvable, i.e. for a Hamiltonian $H' = H_0(\boldsymbol{t}') + H_1(\boldsymbol{U})$ with the same interaction part but a one-particle part that makes it *exactly* solvable. The stationary solutions are obtained (and this is the approximation) *within* the subspace of self-energies $\boldsymbol{\Sigma} = \boldsymbol{\Sigma}(\boldsymbol{t}')$ of that simpler solvable problem that is spanned by varying $\boldsymbol{t}'$. If one takes a single site and connects it to continuous (non-interacting) bath degrees of freedom (another H' choice), one recovers the dynamical mean-field theory (DMFT) [9] or, for a cluster of sites connected to a bath, a cluster variant of DMFT [10].

In the VCA, considered in the following discourse, H' is build up of disconnected clusters, which have their inter-cluster hopping terms removed. In our $T = 0$ approach, the isolated cluster is solved by exact diagonalization. Its Hamiltonian H' includes additional

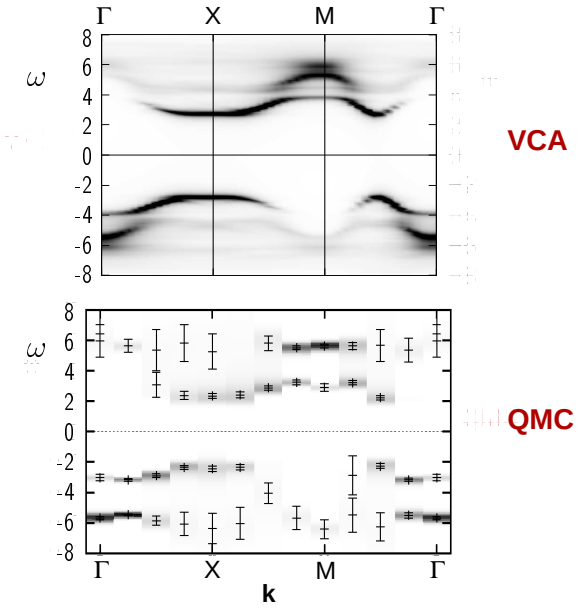

Fig. 1. Upper part: Density plot of the spectral function for the $2D$ Hubbard model at half-filling, $T = 0$ and $U = 8t$ (t: nearest-neighbor hopping) as obtained by the VCA [5]. The lattice is covered by $\sqrt{10} \times \sqrt{10}$ clusters. Bottom: QMC (maximum entropy) result, taken from Ref. [3], for the same parameters but for a finite low temperature $T = 0.1t$ and an isolated 8×8 cluster. Dark (light) areas correspond to large (small) spectral weight.

symmetry-breaking "Weiss" fields [5] to allow for long-range order. The VCA solution is finally obtained as a stationary point determined by $\partial\Omega_{\boldsymbol{t},\boldsymbol{U}}[\Sigma(\boldsymbol{t}')]/\partial\boldsymbol{t}' = 0$. Is this a controlled route to a ($T = 0$) infinite-size approach? To answer this, consider a few "tests":

(i) The VCA correctly reproduces long-range AF order in $2D$ and the absence of this order in $1D$ [5]. This non-trivial test implies that the VCA goes well beyond ordinary mean-field theory.

(ii) An advantage, compared to variational schemes based on wave functions [11], is that the VCA quite naturally gives the one-particle Green's function $\boldsymbol{G}$. Fig. 1 compares the spectral function $A(\boldsymbol{k}, \omega) \propto \mathrm{Im}G(\boldsymbol{k}, \omega)$ of the VCA for the $2D$ Hubbard model at $U = 8t$, half-filling and $T = 0$ with corresponding low-temperature QMC data [3] for an isolated 8×8 cluster. One can clearly see that the VCA, with the lattice covered by $\sqrt{10} \times \sqrt{10}$ clusters, correctly reproduces coherent and incoherent "bands" (known from ARPES data [12]). In particular, the non-trivial proliferation of AF spin correlations from cluster to cluster, which builds up the coherent quasi-particle "band" is obviously correctly embedded in the VCA [5]. Similar calculations have been performed for the spectral function $A(\boldsymbol{k}, \omega)$ of the hole- and electron-doped Hubbard model [6, 7]. The characteristically different doping dependencies give rise to different Fermi-surface evolutions upon doping.

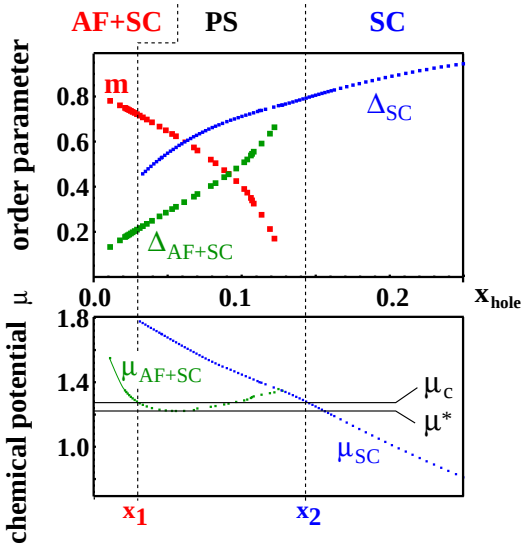

Fig. 2. Antiferromagnetic and superconducting order parameters, m and Δ, and chemical potential μ as functions of hole doping x. Δ and μ are plotted for the AF+SC (green, $\Delta_{\rm AF+SC}$, $\mu_{\rm AF+SC}$) as well as for the pure SC homogeneous solutions (blue, $\Delta_{\rm SC}$, $\mu_{\rm SC}$). Note that Δ is scaled by a factor 10 for convenience. For $x < x_1$ the system exhibits a coexistence of AF and dSC order. Phase separation (PS) occurs between the doping levels x_1 and x_2. For $x > x_2$ pure dSC is realized. In the phase separation region $x_1 < x < x_2$, the homogeneous solutions become unstable, and the system prefers to separate into a mixture of two densities corresponding to x_1 and x_2. The chemical potential μ_c is determined by the Maxwell construction shown in the figure. At μ^* the slope of the AF+SC solution changes sign.

Furthermore, the single-particle excitations provide insight into the characteristic differences in the ground-state phase diagram for hole- and electron-doping [7].

(iii) To test the stability of the homogeneous phases with respect to phase separation (PS), we consider a reference system H' of isolated 2×2 clusters where, in addition to the two symmetry-breaking terms (Weiss fields) $H'_{\rm AF}$ and $H'_{\rm SC}$, a term H'_{local} is optimized within the variational procedure [7]. $H'_{local} = \varepsilon \sum_{i\sigma} n_{i\sigma}$ describes a shift ε of the chemical potential in the cluster with respect to the physical chemical potential μ. The use of the additional variational parameter ε is required in order to have a consistent treatment of the particle density. The optimization of ε has to be done simultaneously with the optimization of the parameters $h_{\rm AF}$ and $h_{\rm SC}$, namely the staggered magnetic field in the term $H'_{\rm AF}$ and the nearest-neighbor d-wave pairing field $h_{\rm SC}$ in the term $H'_{\rm SC}$. Notice that the Weiss fields $h_{\rm AF}$ and $h_{\rm SC}$ are different from the corresponding order parameters m and Δ plotted in Figs. 2 and 3. Quite generally, however, a nonvanishing stationary value for the Weiss fields produces a nonvanishing order parameter, although the latter can be much smaller.

The phase diagram for the Hubbard model with $U = 8t$ and next-nearest-neighbor hopping $t_{n.n.n} = -0.3t$, obtained with our calculation, is plotted in Fig. 2 for the hole-doped and in Fig. 3 for the electron-doped case. In the upper part of each figure, we display the AF (m) and dSC (Δ) order parameters as a function of doping x. In the lower part of the figures, the chemical potential μ is plotted as a function of x.

Let us discuss hole doping first (see Fig. 2). For dopings x below a critical value x_1 we find a homogeneous symmetry-broken state in which both, the AF as well as the dSC order parameter m and Δ are non-zero. This corresponds to a phase AF+SC where AF and dSC order microscopically and coherently coexist. A homogeneous state with pure dSC ($m = 0$ and $\Delta > 0$) is obtained for dopings $x > x_2$.

Fig. 2 also shows Δ and μ for the homogeneous AF+SC and SC phases in the range $x_1 < x < x_2$. Here, however, these phases are thermodynamically unstable. For dopings x with $x_1 < x < x_2$, macroscopic phase separation between the two phases occurs. In practice, doping-dependencies are calculated by varying the chemical potential μ. Following up the grand potentials for the two homogeneous phases as functions of μ, i.e. $\Omega_{\rm AF+SC}(\mu)$ and $\Omega_{\rm SC}(\mu)$, it is found (see Ref. [7] for details) that there is a crossing at a critical chemical potential $\mu = \mu_c$ (at this point the AF order parameter m is still nonzero). Thus, the transition is first order as a function of μ. At the transition point μ_c, the dopings corresponding to the AF+SC and to the SC phase, $x_{\rm AF+SC}$ and $x_{\rm SC}$, are different. Consequently, there is a jump $\Delta x \equiv x_{\rm AF+SC} - x_{\rm SC}$ at μ_c,

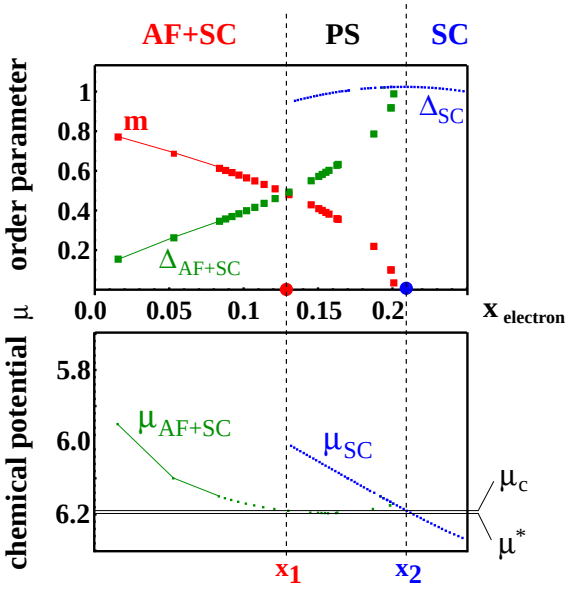

Fig. 3. The same as Fig. 2 but for electron doping. Note the enhanced robustness of the AF state and the strongly reduced scale $\Delta\mu \equiv (\mu^* - \mu_c)$ as compared to hole doping.

indicating phase separation between a weakly doped AF+SC and a higher doped SC phase.

Due to the inclusion of $H'_{\rm local}$, μ_c can *equivalently* be obtained by a Maxwell construction. This is shown in Fig. 2 where, in the lower panel, μ is plotted as a function of x. Here, phase separation is signaled by the fact that the $\mu(x)$ is not a monotonous function. The Maxwell construction shown in the figure then identifies the two dopings x_1 and x_2 into which the system tends to phase separate, as well as the chemical potential μ_c in the phase-separated state. In Fig. 2, μ^* is the point where the slope of $\mu(x)$ changes sign. For $\mu < \mu^*$ the AF+SC solution ceases to exist

Let us now discuss the electron-doped case. While the phase diagrams in Figs. 2 and 3 are *qualitatively* similar, the phase in which long-range AF order is realized is spreading to significantly larger doping values in the electron-doped case, in overall agreement with the experimental situation. Another important difference concerns the energy scale for phase separation, i.e. $\Delta\mu \equiv (\mu^* - \mu_c)$. As one can see from the comparison between Figs. 2 and 3, $\Delta\mu$ is an order of magnitude larger in the hole-doped case. In Ref. [7] it is argued that this can explain the different pseudogap and SC transition scales in hole- and electron-doped materials. This may give support to theories [13] which are based on the idea that fluctuations of the competing phases, or of the related order parameters, are responsible for the pseudogap phenomenon.

In order to resolve the relevant small energy scale, it is necessary to evaluate Ω as well as its stationary points with high accuracy. Furthermore, the inclusion of the chemical potential shift term H'_{local} considerably complicates the variational optimization. For the rather small clusters of size 2×2 used here, the reference system can be treated by full diagonalization and the frequency integrals, which are implicit in Eq. (2) [8], can be carried out by means of a sum over the negative poles of the Green's functions. Sénéchal et. al. [6] have considered clusters up to 10 sites and report similar results for $x \approx 0$ but, without the inclusion of H'_{local}, one cannot reliably test the stability of the homogeneous phases against phase separation. Note that the transition from the AF+SC to the SC phase may appear as continuous as a function of x if phase separation is not taken into account.

In conclusion, there has been substantial recent progress in relating the "high-energy" physics of the Hubbard model and its variants to the low-energy physics of the competing phases AF, dSC, charge inhomogenities, etc. This progress is due to the development of quantum-cluster theories, such as the VCA discussed here but also due to cluster extensions of the DMFT, such as the dynamical cluster approximation (DCA) [14, 15]. Within these cluster approaches, characteristic difficulties have been encountered: The latest impressive work using the DCA by Maier et. al. performed a systematic cluster-size study of dSC in the $2D$ Hubbard model [14]. In clusters large enough (up to 26 sites) converged results point to a finite-T instability to dSC. Because of the QMC minus-sign problem, however, results were limited to $U = 4t$, where the typical energy separation in U and the magnetic energy scale of the HTSC is not yet achieved. On the other hand, the VCA studies reviewed here, are clearly not yet converged with respect to the cluster size, as one can read off from Fig. 1 in Ref [6]. Cluster convergence is, at least in principle, also possible within the VCA. With increasing cluster size longer-ranged correlations are included exactly. This, however, necessarily implies to use stochastic (QMC) methods as solvers for the cluster reference system.

One of us (WH) would like to acknowledge the hospitality of the Kavli Institute for Theoretical Physics in Santa Barbara, where part of this work was finished (supported by Nat. Sc. Found. Grant No. PHY99-0794). We would like to thank D. J. Scalapino for many useful discussions. This work was also supported by the DFG Forschergruppe 538, by the KONWIHR supercomputing network in Bavaria, and by the Doctoral Scholarship Program of the Austrian Academy of Sciences.

References

[1] P. W. Anderson, Science 235. 1196 (1987), see also D. J. Scalapino, Phys. Rep. 250, 330 (1995)

[2] M. Imada, A. Fujimori and Y. Tokura, Rev. Mod. Phys. 70, 1039 (1998)

[3] R. Preuss, W. Hanke, C. Groeber and H. G. Evertz, Phys. Rev. Lett. 79. 1122 (1997) and R. Preuss, W. Hanke and W. v.d. Linden, PRL 75, 1344 (1995), and references therein

[4] M. Potthoff, M. Aichhorn and C. Dahnken, Phys. Rev. Lett 91, 206402 (2003)

[5] C. Dahnken, M. Aichhorn, W. Hanke, E. Arrigoni and M. Potthoff, Phys. Rev. B 70, 245110 (2004)

[6] D. Sénéchal et. al., Phys. Rev. Lett 94 (2005) 156404

[7] M. Aichhorn and E. Arrigoni, cond-mat/0502047

[8] M. Potthoff, Eur. Phys. J. B 32, 429; 36, 335 (2003)

[9] A. Georges et. al., Rev. Mod. Phys. 68, 13 (1996)

[10] G. Kotliar et. al., Phys. Rev. Lett. 87, 186401 (2001)

[11] A. Paramekanti et. al., Phys. Rev. B 70, 054504 (2004)

[12] see, e.g., A. Damascelli, Z. Hussain and Z.X. Shen, Rev. Mod. Phys. 75, 474 (2004)

[13] E. W. Carlson, V. J. Emery, S. A. Kivelson and D. Orgad, in The Phys. of Superconductivity, ed. by K. H. Bennemann (Springer, Berlin, 2003), Vol I

[14] T. A. Maier, M. Jarrell, et. al., cond-mat/0504529

[15] A. Macridin, M. Jarrell, Th. Maier, cond-mat/0506148